Power electronics cooling by flow boiling of R134a in parallel copper microchannels

Criscuolo, Gennaro; Kærn, Martin R.; Markussen, Wiebke B.

Published in:
Proceedings of ECOS 2020: 33rd International Conference on Efficiency, Cost, Optimization, Simulation and Environmental Impact of Energy Systems

Publication date:
2020

Document Version
Publisher's PDF, also known as Version of record

Power electronics cooling by flow boiling of R134a in parallel copper microchannels

Gennaro Criscuolo[a], Martin R. Kærn [b] and Wiebke B. Markussen[c]

*[a] Technical University of Denmark, Mechanical Engineering, Lyngby, Denmark, gcri@mek.dtu.dk, **CA***
[b] Technical University of Denmark, Mechanical Engineering, Lyngby, Denmark, pmak@mek.dtu.dk
[c] Technical University of Denmark, Mechanical Engineering, Lyngby, Denmark, wb@mek.dtu.dk

Abstract:

Power electronics represent a core component of many energy-management technologies, such as power drives used in wind turbine or electric vehicles. This type of circuitry has increased its cooling needs over the years and currently new and more efficient cooling solutions are researched to accommodate the next generation of power devices. Flow boiling of refrigerants in very narrow channels is recognized as a technical solution with a high potential for very efficient and uniform cooling. The current work presents the description of an experimental setup to test the flow boiling of refrigerants in various micro-geometries. A set of 25 parallel channels with a nominal width of 300 µm and a nominal height of 1200 µm was tested. Boiling curves for R134a are shown for nominal mass fluxes of 180 kg $s^{-1}m^{-2}$ and 880 kg $s^{-1}m^{-2}$, evaporating temperature of 30°C at the outlet and inlet flow sub-cooling of 6°C. The maximum footprint heat flux dissipated amounts to 600 W cm^{-2} for the highest mass flow rate tested. The measurements are supported by high-speed visualization of the flow inside the channels.

Keywords:

Flow boiling, microchannel, thermal management, power electronics

1. Introduction

Very narrow channels can support a lot of cooling applications, due to their capability of increasing the heat transfer surface in very compact spaces [1]. In particular, the cooling of microchips could take advantage of micro-geometries, especially if they are combined with heat removal by boiling. Heat transport capabilities of evaporating flows are greater than single-phase ones, which currently represent the industrial state-of-art. Localized cooling by boiling flows can guarantee a better temperature uniformity on micro-chips, which is practically translated into less spatial gradient in temperature, improving electronics reliability and lifetime. High temperatures are recognized as the main cause of chip failure, whose life span is strictly correlated to the working temperature [2]. Power electronics is a key component for the future energy systems, since it is at the core of many power-management technologies. This has paved the way to a strong industrial and research interests.

Using flow boiling for cooling applications can guarantee lower mass flow rates compared to the single-phase counterpart, improve temperature uniformity and increase the amount of heat that can be dissipated at the same temperature level.

The present study investigates experimentally the thermal performances of R134a flowing into a copper multi-microchannel heat sink made of 25 channels with a hydraulic diameter of 480 µm. The results are described in terms of boiling curves at a nominal saturation temperature of 30 °C.

2. Literature review

The continuous miniaturization in electronics has strongly promoted the studies of localized cooling solutions that can handle high heat fluxes, in the range of hundreds of W cm^{-2}. Research in heat transfer performance of microchannels started with the study by Tuckermann and Pease [3], where

heat fluxes up to 790 W cm^{-2} were predicted. Since then, microchannels have been an object of intense research and several review articles were published. A comprehensive review can be found in [4].

While single-phase flow is considered to obey the laws of conventional channels [5], boiling in the micro-geometrical domain shows considerable effects due to the dominance of surface forces over body forces and confinement effects. In particular, confinement effects may be responsible for instabilities in the flow distribution in the parallel microchannels, thus complicating the analysis of the physical problem [6]. Stratified flow is also not observed for these geometries. Moreover, flow reversal is recognized as a potential source for premature dry-out of the heat transfer area [7].

Many investigations on flow boiling in microchannels [8] took place and currently no general agreement is reached on the dominating heat transfer mechanism and suitable design correlations for the heat transfer coefficient and pressure drop. Measurements in parallel microchannels can provide many challenging elements, mainly related to the complicacy of placing sensors inside all the parallel channels [9].

Table 1: listing of channel geometries for recent studies in straight multi-microchannel heat sinks with R134a.

Year	ID	N	H [µm]	W [µm]	Dh [µm]	H/W
2016	[10]	27	470	382	421	1.2
	[11]	21	930	335	493	2.8
2017	[12]	25	700	300	420	2.3
2018	[13]	27	470	382	421	1.2

Water is a good cooling medium for power electronics, due to its low cost and good heat transfer properties. However, refrigerants are also investigated [14] as they can withstand low stocking temperatures and may be more suitable for the integration of the chip as a heat source into heat recovery processes. Table 1 reports the geometries studied previously that involved the use of copper microchannels and R134a, as they were the main object of the investigation in the present study.

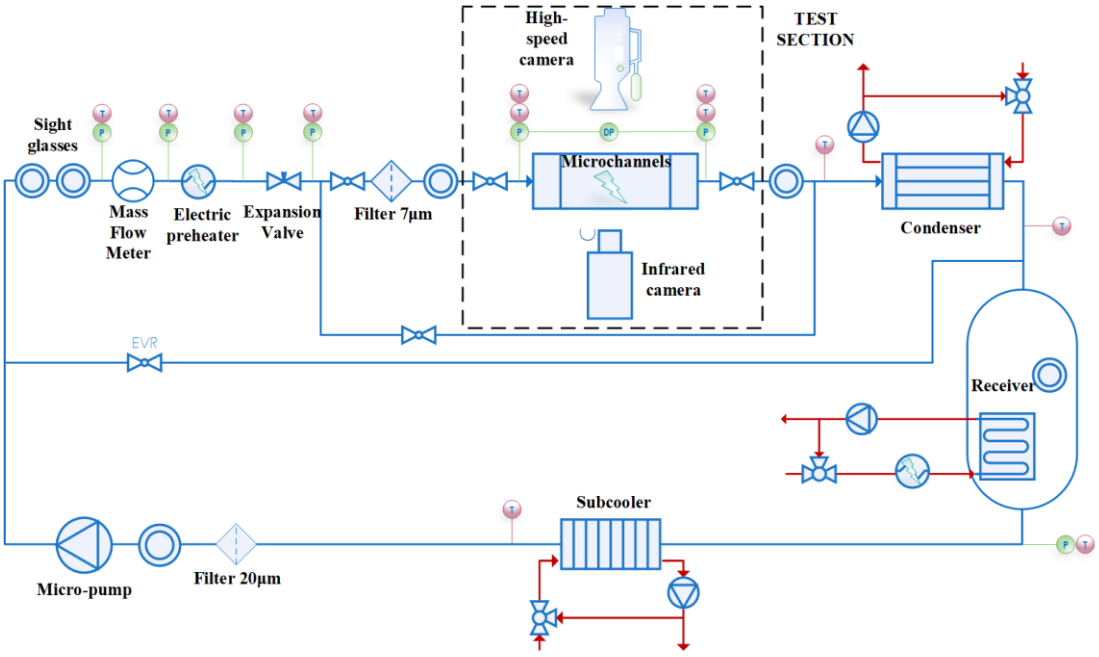

Figure 1: schematic diagram of the experimental setup. Test section highlighted by the dotted box.

3. Experimental setup

A schematic of the experimental setup used for the investigation is reported in Figure 1. The experimental conditions for the present study are reported in Table 2. All the measurements needed to evaluate the boiling curves of the chosen geometry were conducted in the test section while the remaining part of the setup is used for refrigerant flow conditioning. The main components used in the setup are listed in Table 3.

In the flow conditioning loop, a gear pump with a frequency driver was employed to adjust the mass flow rate inside the parallel channels. Filters of 2 different sizes were used to avoid channels clogging by micro-particles possibly dispersed into the liquid refrigerant. Sub-cooling at the inlet of the test section was controlled by an electrically powered preheater. A needle valve before the test section was employed to increase the stiffness of the system and minimize flow oscillations during evaporation at low mass flow rates, if any. After evaporation takes place inside the test section, the flow is condensed and accumulated into a receiver. The receiver is equipped with an internal coil to provide cooling and heating and eventually control the pressure inside the system. Both the test section and the flow conditioning loop were instrumented with temperature, pressure and mass flow sensors in order to calculate the thermodynamic state of the refrigerant at each point of interest. Together with the loop, a high-speed camera was used to visualize the flow from the top of the test section, while an IR camera was used to measure the wall temperature at the bottom of the microchannels.

Table 2: experimental conditions of the present investigation.

Value	Units	Min	Max
G	kg $s^{-1}m^{-2}$	176	877
q_b	W cm^{-2}	20	600
$T_{sat,out}$	°C	30	30
DT_{sc}	°C	5	7

Table 3: main components list and use.

Component	Model	Use
Pump + Drive	Tuthill, D_serie, 0.38	Flow rate adjustment
Flow Meter	Micromotion CMF010	Flow rate measurement
Expansion valve	Danfoss REG-SA 10-40	System control
Filter	Hamlet 2 μm - 20 μm	Avoid clogging
HS Camera	Fastcam Nova	Flow visualization
IR Camera	FLIR A655	Temperature distribution

3.1. Test section

The test section comprised of a microchannel evaporator placed into a steel assembly used to convey the refrigerant flow from the main piping to the microchannels inlet. An exploded view is depicted in Figure 2. Microchannels were machined in a high-purity copper block, over a nominal square area of 1 cm^2. The nominal width of the channels was 300 μm, while the nominal height was 1200 μm. Channels spacing amounted to 100 μm, thus resulting in a set of 25 parallel channels. As the heat transfer performance is very sensitive to the hydraulic diameter of the passage, channels were measured with a confocal microscope. Exact dimensions and standard deviation are found in

Table 4. Geometrical characterization of the channels took place by repeated measurements at 5 different locations on the microchannels footprint area (4 measurements at the corners and 1 in the center). Average surface roughness, measured from a sample piece realized with the same manufacturing process of the channels, amounted to 0.53 μm (Ra parameter), with a standard deviation of 19%.

The inlet and outlet manifold to the channels were also machined into the copper block and insulated with peek inserts: due to high thermal conductivity of copper, subcooled boiling is likely to occur. In order to avoid this phenomenon to bias the data, inserts manufactured with low-thermal conductivity materials were used. Avoidance of subcooled boiling before the inlet of the channels was confirmed by flow visualization. On the bottom of the copper block, a custom-made micro-heater was soldered and it acted as a known heat flux surface for the channels. The top of the channels was covered with a borosilicate glass, which allowed flow visualization.

The micro-heater was manufactured with a 1 μm deposition of platinum on a silicon layer of 350 μm. The platinum was deposited in a serpentine geometry, with ending pads to connect to the power supply. Inside the serpentine, 4 RTDs were realized by the same deposition technology. The RTDs were calibrated in a temperature bath and later used to calibrate the IR camera.

Test methodology consisted of setting known conditions at the inlet of the channels in terms of pressure, sub-cooling and mass flow rate and then apply a known heat flux on the microchip – thus producing boiling inside the channels. Recordings were taken for a duration of 2 minutes at a sampling frequency of 10 Hz.

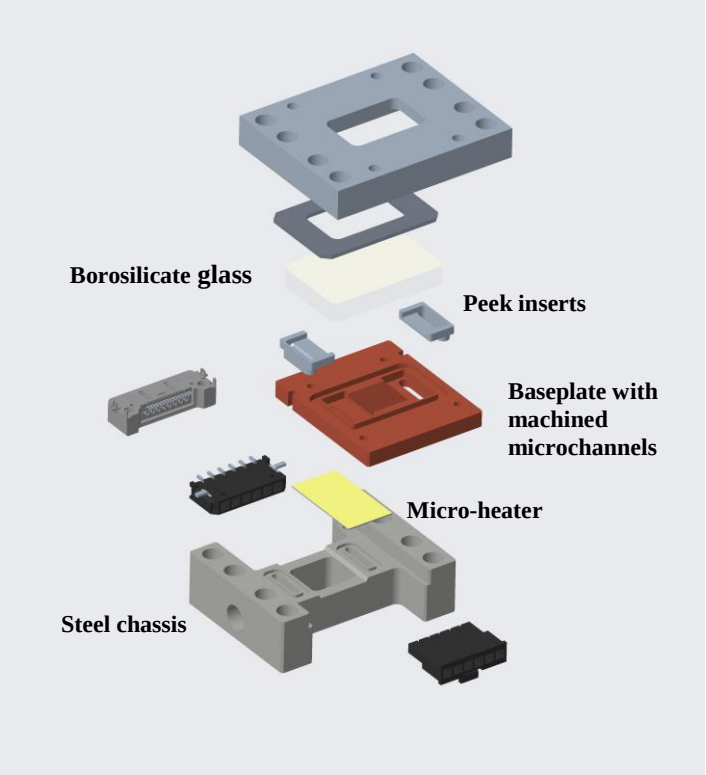

Figure 2: exploded view of the test section

Table 4: geometry of the investigated channels.

Quantity	Average value [mm]	Standard deviation [mm]
Height	1.193	0.0005
Width	0.282	0.002
Spacing	0.116	0.003

4. Data reduction

The present work investigates the boiling performance of R134a during forced motion inside microchannels. The investigation is characterized by the generation of boiling curves, which describes the absorbed heat flux versus the wall temperature, i.e. the temperature at the bottom of the channels T_{wall}. Test conditions are described by channel average thermodynamic pressure, flow sub-cooling at the inlet, channel average mass flux G and base heat flux q_b. The following describes how each term was calculated from the measured quantities, underlying the assumed hypothesis.

Channel mass flux, G: the average channel mass flux was computed under the hypothesis of uniform flow distribution, according to Eq. (1),

$$G = \frac{\dot{m}}{NA_{ch}} \qquad (1)$$

where $\dot{m}$ is the measured mass flow rate, N is the number of parallel channels and NA_{ch} is the overall section of refrigerant flow. According to a visual inspection by the HS camera videos, flow maldistribution did not seem evident for most of the tests. Only at the lowest mass flux and the highest heat flux, instabilities in the mass flow rate were observed, due to large vapor generation inside the channels [7].

Base heat flux, q_b: it is the heat flux that reaches the bottom of the channels and differs from the one generated on the chip by the heat flux lost to the environment. Radiation losses were neglected. The base heat flux q_b was calculated according to Eq. (*2*),

$$q_b = \frac{IV}{A_b} - q_{lost} \qquad (2)$$

where I and V are, respectively, the current and the voltage of the power supply and A_b is the nominal footprint area of the micro-heater, equal to 1 cm^2. The base heat flux entering the copper block is mainly absorbed by the evaporating refrigerant and a small part is dispersed to the ambient, q_{lost}. Heat losses to the ambient were evaluated by separate tests with vacuum and single-phase flow.

Wall temperature, T_{wall} : wall temperature is recognized as being the temperature at the bottom of the channels, calculated from the IR camera measurement T_b according to Eq.(3):

$$T_{wall} = T_b - \frac{q_b t}{k} \qquad (3)$$

where q_b is the heat flux at the microchannel base, t is the conduction thickness between the micro-heater and the bottom of the channels and k is the equivalent thermal conductivity of the conduction thickness. The nominal conduction thickness comprised a layer of silicon of 350 μm, a layer of tin of 100 μm and a copper substrate of 2580 μm.

The data reduction methodology has been validated by measuring the heat transfer performance of single-phase flows in the laminar flow regime, whose heat transfer coefficient is well-known. The comparison between the measured data and those predicted by Shah and London correlation [15] gave deviations lower than 15%.

5. Experimental results

Boiling curves for mass fluxes of 176 kg $s^{-1}m^{-2}$ and 877 kg $s^{-1}m^{-2}$ are reported in Figure 3. Saturation temperature at the outlet of the channels was kept constant at 30 °C. For both mass fluxes, the heat fluxes absorbed by the refrigerant grows with the wall temperature. For both mass fluxes, the trend is not linear, thus suggesting a heat transfer performance which is not constant with the heat flux. At the highest mass flow rate, the calculated output quality resulted to be 0.37, while for the lowest mass flow rate the outlet condition at the highest heat flux was superheated vapor. This can be seen by the

almost horizontal trend of the boiling curve at 176 kg $s^{-1}m^{-2}$, which indicates an extremely bad heat transfer process, mainly due to a large presence of vapor in the channels. These observations are supported by flow visualization, which confirms both the absence of subcooled boiling before the channels inlet and the large presence of refrigerant vapor at very high heat fluxes. Another observation is related to the heat flux dissipated by the channels, which shows a difference between the two mass fluxes only at wall temperatures larger than 45 °C. At low heat fluxes (bubbly flow), no clear difference can be observed between the mass fluxes. As a general remark, the indicated channel mass flux should be considered as an indicator of the mass flow rate running through the system. Due to the high number of channels and the absence of inlet restrictors, flow distribution among channels might experience small non-uniformities, whose extent is rather difficult to evaluate quantitatively from flow visualization. This is a practical limit with which all the published studies dealt with.

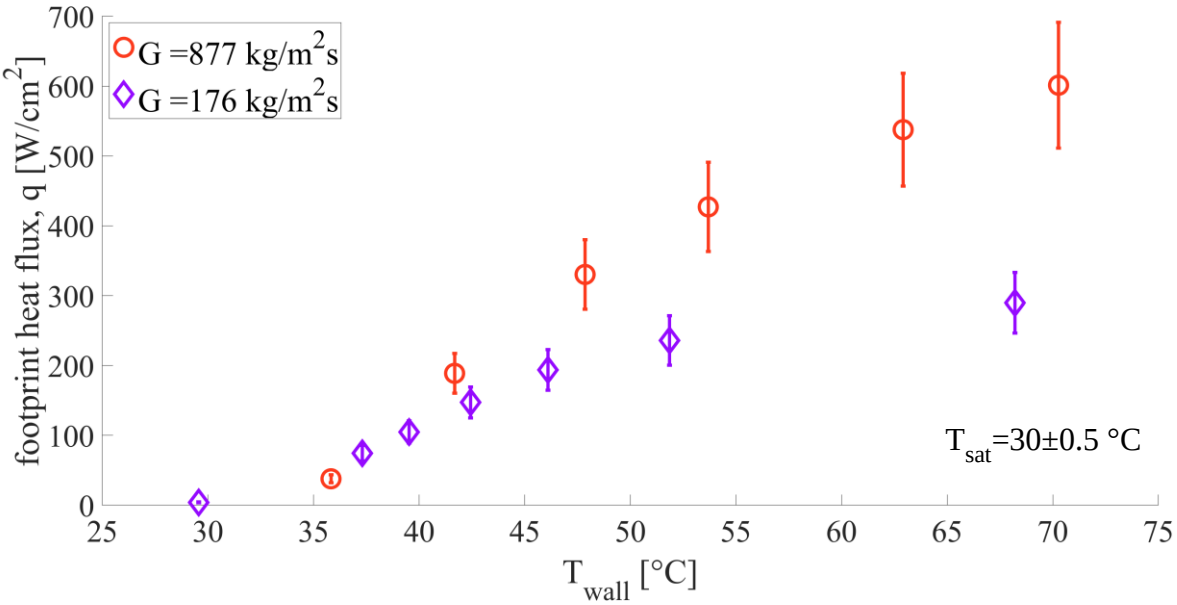

Figure 3: boiling curves for 877 kg $s^{-1}m^{-2}$ and 176 kg $s^{-1}m^{-2}$, T_{sat}= 30±0.5 °C.

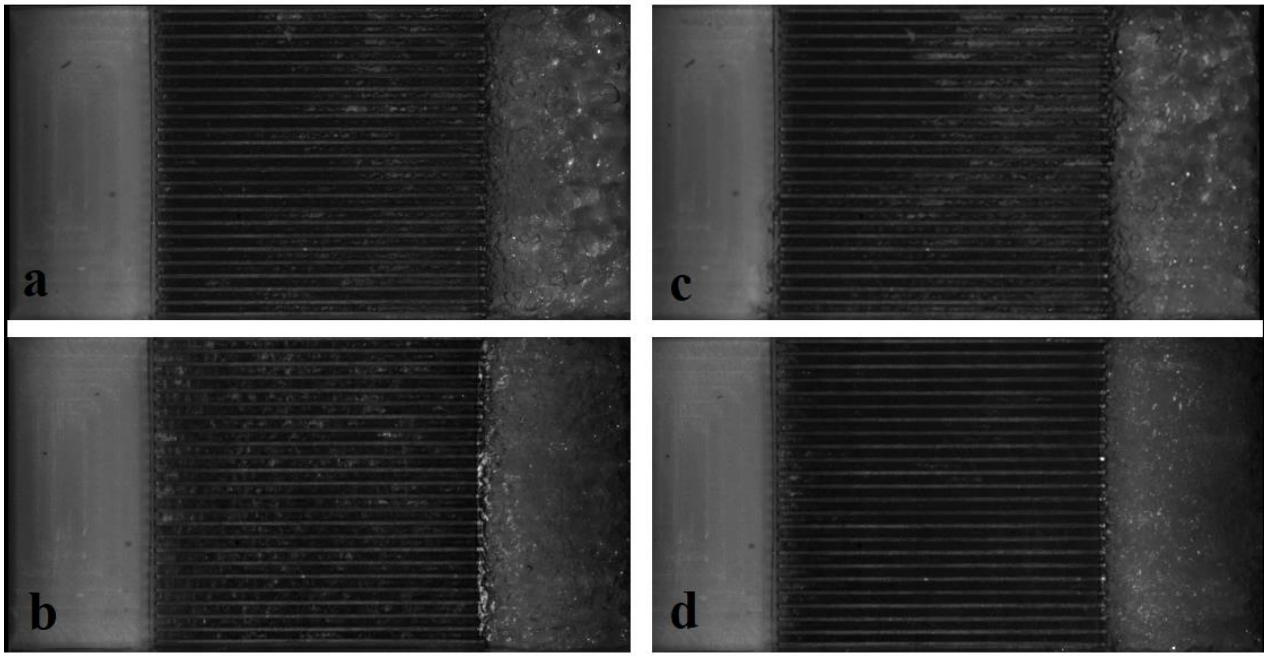

Figure 4: flow visualization from top of the microchannels. T_{wall} ~45°, a) G = 176 kg $s^{-1}m^{-2}$, b) G = 877 kg $s^{-1}m^{-2}$; T_{wall} ~65°, c) G =176 kg $s^{-1}m^{-2}$, d) G=877 kg $s^{-1}m^{-2}$. Large vapour formation (grey area) in c) produces an almost horizontal boiling curve in Figure 3 for G =176 kg $s^{-1}m^{-2}$;

6. Discussion

As previously described, the heat transfer performance is affected by the mass flow rate only at higher wall temperatures. This observation can be interpreted as an indicator of the dominance of convective effects in the heat transport process only for the higher heat fluxes tested, i.e. when vapor presence becomes dominant in the flow. Flow visualization for the two conditions is displayed in Figure 4. It can be otherwise considered that at low vapor qualities, the heat transfer process is dominated by nucleation, thus not resulting in relevant differences between the two conditions and mass flow rates. A similar effect of the mass flow rate was also observed in [16] for silicon microchannels and [10], [12], [13] for copper microchannels. In particular, for a saturation temperature of 23 °C, a hydraulic diameter of 421 μm, a wall superheat of 4 °C and a mass flux of 150 kg $s^{-1}m^{-2}$, [10] reports a local heat flux of approximately 8 W cm^{-2}, while for the current study a value of 6.8 W cm^{-2} can be estimated from Figure 3, when the mass flux is 176 kg $s^{-1}m^{-2}$. The differences in values can be accounted for by considering the slightly different test conditions and experimental uncertainty. Referring to the highest mass flux tested in this study, similar conditions are tested in [13]. It is reported that a local heat flux of approximately 43 W cm^{-2} is obtained for a saturation temperature of 28 °C, a hydraulic diameter of 421 μm, a wall superheat of 6 °C and a mass flux of 1000 kg $s^{-1}m^{2}$. However, for the current study, a value of approximately 15 W cm^{-2} can be estimated from Figure 3, when the mass flux is 877 kg $s^{-1}m^{-2}$. In these conditions, the deviation is larger compared to the value reported in [13] and differences in test conditions can not support the deviation. In general, more data points need to be taken and analysed in order to comprehensively describe the heat transfer process and make a complete comparison with other studies.

7. Conclusion

The present manuscript reports preliminary data on the heat transfer behaviour of R134a in straight copper microchannels. Nominal channels height and width were, respectively, 1200 μm and 300 μm. Mass flux resulted to affect the performance only at wall superheat higher than 15 °C, while the performance were similar for relatively lower superheat values. This effect is related to the average vapour quality inside the channels. In summary, 600 W were dissipated with a temperature superheat of 70 °C for the 877 kg $m^{-2}s^{-1}$ case. Nucleate boiling was recognized as the dominating heat transfer mechanism at low heat flux. The analysis was supported by flow visualization images. However, further experiments are needed in order to provide better foundations to the assumption on dominating heat transfer mechanism.

References

[1] T. G. Karayiannis and M. M. Mahmoud, "Flow boiling in microchannels: Fundamentals and applications," *Appl. Therm. Eng.*, vol. 115, pp. 1372–1397, 2017, doi: 10.1016/j.applthermaleng.2016.08.063.

[2] S. T. Kadam and R. Kumar, "Twenty first century cooling solution: Microchannel heat sinks," *Int. J. Therm. Sci.*, vol. 85, pp. 73–92, 2014, doi: 10.1016/j.ijthermalsci.2014.06.013.

[3] D. B. Tuckerman and R. F. W. Pease, "High-performance heat sinking for VLSI," *IEEE Electron Device Lett.*, vol. 2, no. 5, pp. 126–129, 1981, doi: 10.1109/EDL.1981.25367.

[4] A. S. Dalkılıç, "a Review of Flow Boiling in Mini and Microchannel for Enhanced Geometries," *J. Therm. Eng.*, vol. 4, no. 3, pp. 2037–2074, 2018, doi: 10.18186/journal-of-thermal-engineering.411437.

[5] G. Hetsroni, A. Mosyak, E. Pogrebnyak, and L. P. Yarin, "Fluid flow in micro-channels," *Int. J. Heat Mass Transf.*, vol. 48, no. 10, pp. 1982–1998, 2005, doi:

10.1016/j.ijheatmasstransfer.2004.12.019.

[6] Y. K. Prajapati and P. Bhandari, “Flow boiling instabilities in microchannels and their promising solutions – A review,” *Exp. Therm. Fluid Sci.*, vol. 88, no. April, pp. 576–593, 2017, doi: 10.1016/j.expthermflusci.2017.07.014.

[7] S. M. Kim and I. Mudawar, “Review of two-phase critical flow models and investigation of the relationship between choking, premature CHF, and CHF in micro-channel heat sinks,” *Int. J. Heat Mass Transf.*, vol. 87, pp. 497–511, 2015, doi: 10.1016/j.ijheatmasstransfer.2015.04.012.

[8] G. Ribatski, “A critical overview on the recent literature concerning flow boiling and two-phase flows inside micro-scale channels,” *Exp. Heat Transf.*, vol. 26, no. 2–3, pp. 198–246, 2013, doi: 10.1080/08916152.2012.737189.

[9] G. L. Morini, “The Challenge to Measure Single-phase Convective Heat Transfer Coefficients in Microchannels,” *Heat Transf. Eng.*, vol. 7632, pp. 1–16, 2018, doi: 10.1080/01457632.2018.1442290.

[10] P. Thiangtham *et al.*, “An experimental study on two-phase flow patterns and heat transfer characteristics during boiling of R134a flowing through a multi-microchannel heat sink,” *International Journal of Heat and Mass Transfer*, vol. 98. pp. 390–400, 2016, doi: 10.1016/j.ijheatmasstransfer.2016.02.051.

[11] V. V. Kuznetsov and A. S. Shamirzaev, “Flow Boiling Heat Transfer of Refrigerant R-134a in Copper Microchannel Heat Sink,” *Heat Transf. Eng.*, vol. 37, no. 13–14, pp. 1105–1113, 2016, doi: 10.1080/01457632.2015.1111103.

[12] E. M. Fayyadh, M. M. Mahmoud, K. Sefiane, and T. G. Karayiannis, “Flow boiling heat transfer of R134a in multi microchannels,” *Int. J. Heat Mass Transf.*, vol. 110, pp. 422–436, 2017, doi: 10.1016/j.ijheatmasstransfer.2017.03.057.

[13] A. S. Dalkılıç, C. Özman, K. Sakamatapan, and S. Wongwises, “Experimental investigation on the flow boiling of R134a in a multi-microchannel heat sink,” *Int. Commun. Heat Mass Transf.*, vol. 91, no. December 2017, pp. 125–137, 2018, doi: 10.1016/j.icheatmasstransfer.2017.12.008.

[14] C. B. Tibiriçá and G. Ribatski, “Flow boiling in micro-scale channels-Synthesized literature review,” *Int. J. Refrig.*, vol. 36, no. 2, pp. 301–324, 2013, doi: 10.1016/j.ijrefrig.2012.11.019.

[15] R. K. Shah and A. L. London, “Rectangular Ducts,” *Laminar Flow Forced Convect. Ducts*, pp. 196–222, 1978, doi: 10.1016/b978-0-12-020051-1.50012-7.

[16] H. Huang, N. Borhani, and J. R. Thome, “Experimental investigation on flow boiling pressure drop and heat transfer of R1233zd(E) in a multi-microchannel evaporator,” *Int. J. Heat Mass Transf.*, vol. 98, pp. 596–610, 2016, doi: 10.1016/j.ijheatmasstransfer.2016.03.051.